Appl. Phys. B 87, 469–473 (2007)
DOI: 10.1007/s00340-007-2629-3

Applied Physics B
Lasers and Optics

K. LU[1]
W. ZHAO[1]
Y. YANG[1]
Y. YANG[1]
M. ZHANG[1]
R.A. RUPP[2,✉]
M. FALLY[2]
Y. ZHANG[3]
J. XU[4]

One-dimensional incoherently coupled grey solitons in two-photon photorefractive media

[1] State Key Laboratory of Transient Optics and Photonics, Xi'an Institute of Optics and Precision Mechanics, Chinese Academic of Sciences, Xi'an 710068, P.R. China
[2] Vienna University, Physics Faculty, Nonlinear Physics Group, Boltzmanngasse 5, 1090 Wien, Austria
[3] Department of Electronic Science and Technology, Xi'an Jiaotong University, Xi'an 710049, P.R. China
[4] Department of Physics, Nankai University, Tianjin 300071, P.R. China

Received: 4 September 2006/Revised version: 31 January 2007
Published online: 25 April 2007 •

ABSTRACT We show that grey solitons, grey–grey soliton pairs, and multi-component grey solitons can be realized in two-photon photorefractive media. The results for soliton pairs and multi-component solitons are derived under the assumption that the carrier beams share the same polarization, wavelength, and are mutually incoherent.

PACS 42.65.Tg; 42.65.Hw; 42.70.Nq

1 Introduction

Spatial solitons have attracted a great deal of attention because of their possible applications for optical switching and routing [1–22]. Besides these electromagnetic field solitons also refractive index solitons have been investigated in photorefractive (PR) media [23]. Several generic types of wave-field PR solitons have been predicted and observed thus far, including quasi-steady-state solitons [1, 2], screening solitons [3–6], photovoltaic solitons [7–10], screening-photovoltaic solitons [11–13], and spatial solitons in PR centrosymmetric materials [14, 15] and in anisotropic nonlinear media [16, 17], all of which result from the single-photon photorefractive effect. Very recently, single beam bright and dark solitons in two-photon photorefractive materials have been predicted, which result from the two-photon PR effect [18]. On the other hand, grey solitons and grey–grey soliton pairs have been predicted for screening solitons [4, 19–21] and screening-photovoltaic solitons [22] that result from the single-photon PR effect. Consequently, it would be of interest to explore whether grey solitons, grey–grey soliton pairs, and multi-component grey solitons can be realized in two-photon photorefractive crystals as well.

In the first part of this paper we derive the intensity version of the fundamental soliton equation. Then we establish a model for the two-photon photorefractive effect. Finally, we show that grey solitons, grey–grey soliton pairs, and multi-component grey solitons can be realized under steady-state conditions by a two-photon photorefractive effect.

✉ Fax: +43-1-4277-51181, E-mail: romano.rupp@univie.ac.at

2 Intensity equation of solitons

In one dimension the propagation of solitons in a perturbed medium is described by the paraxial equation of diffraction [4]:

$$\mathrm{i}\frac{\partial A}{\partial z}+\frac{1}{2k}\frac{\partial^2 A}{\partial x^2}+k_0\Delta n\,A=0\,. \tag{1}$$

Here i is the imaginary unit, A is the optical field amplitude, $k=n_0k_0$, $k_0=\omega_2/c=2\pi/\lambda$, c is the universal speed limit, λ the (vacuum) wavelength, $k_0\Delta n=k(n^2-n_0^2)/2n_0^2$ defines the refractive index perturbation, $n=n(x)$ is the perturbed refractive index and n_0 the unperturbed refractive index. The separation ansatz $A(x,y)=\varphi(x)\psi(z)$ leads to the eigenvalue equation:

$$\left(\frac{1}{2k}\frac{\partial^2}{\partial x^2}+k_0\Delta n\right)\varphi=\Gamma\varphi\,, \tag{2}$$

where Γ is the separation constant and the solution for ψ is $\psi=\exp(\mathrm{i}\Gamma z)$. In photorefractive media Δn is a function of intensity. For the description we introduce here a dimensionless intensity variable $I\propto|\varphi|^2$ normalized by the supremum of the intensity, i.e. we have $0\le I\le 1$. Then (2) has the general form:

$$\left(\frac{\partial^2}{\partial\xi^2}-\frac{1}{4}f(I)\right)\varphi=\frac{1}{4}g\varphi\,, \tag{3}$$

where we introduced the dimensionless space variable $\xi=kx$ and the pertinent soliton (real) propagation constant $g=8\Gamma/k$. Here $f(I)$ is a real function of the intensity and, possibly, of a functional of the intensity. For now, the functional will be considered as a simple constant to be dealt with retrospectively. With the ansatz $\varphi(\xi)=u\exp(\mathrm{i}v)$, where u and v are real functions of ξ, and a dot denoting the derivative with respect to ξ we obtain the relationship:

$$\dot v=\pm\frac{\sqrt{l(l+1)}}{2I}\,. \tag{4}$$

The positive proportionality constant $l(l+1)$ has to be determined from the boundary conditions. For solitons we impose the boundary condition that all derivatives vanish at

infinity. Then from (3) the following fundamental equation for the intensity profile of optical solitons can be deduced:

$$\dot{I} = \pm\sqrt{I\int\left[f(I') + g + \frac{l(l+1)}{I'^2}\right]\mathrm{d}I'}\,. \tag{5}$$

In (5) integration is performed from $I_\infty = I(\xi\to\infty)$ to I (since $\dot{I}(\infty) = 0$).

For all solitons considered here, we assume also $\dot{I}(0) = 0$. Depending on whether the extremum $I_0 = I(0)$ at $\xi = 0$ is a maximum or a minimum we distinguish bright/bright-grey solitons with $I_0 \geq I(x)$ and dark/dark-grey solitons with $I(x) \geq I_0$. As a consequence, for $x < 0$ the positive sign refers to bright/bright-grey, the negative sign to dark/dark-grey solitons, and vice versa for $x > 0$. Because of the normalization we have $I_0 = 1$ for the first type and $I_\infty = 1$ for the latter.

Among these general solitons the so-called dark and bright solitons constitute a special class that fulfill the additional condition of a vanishing centrifugal term, i.e. $l = 0$. As can be seen from (4), these are "plane wave" solitons with constant phase. For the dark soliton with $I_0 = 0$, the condition $l = 0$ is obviously compelling (otherwise the centrifugal term would diverge). Solitons with nonzero centrifugal term will be called (bright- or dark-) grey solitons.

When integrating (5), the new integration constant can be fixed by the value I_0. In addition we may exploit the vanishing second derivative at infinity and the vanishing derivative at $\xi = 0$ to obtain the following relationships:

$$l(l+1) = -I_\infty^2[f(I_\infty) + g] \tag{6}$$

and

$$g = \frac{I_0}{(I_\infty - I_0)^2}\int_{I_0}^{I_\infty} f(I')\,\mathrm{d}I' - \frac{I_\infty}{I_\infty - I_0}f(I_\infty)\,. \tag{7}$$

Thus the constants g and l are fixed by the intensities at the boundaries $\xi = 0$ and $\xi\to\infty$.

As a rule, the resulting differential equation, (5) with (6) and (7), has no analytic solution and needs to be solved by numerical methods.

3 Material equations for two-photon photorefraction

In the next step we derive the function $f(I)$ for an electro-optic two-photon photorefractive medium with an external electric bias voltage V_{ext} applied parallel to its crystallographic c axis. A so-called gating beam illuminates the medium homogeneously along the x (or y) direction with constant intensity I_1, the x direction being parallel to the crystallographic c axis. A second optical beam, the so-called soliton beam, is polarized along the c axis, propagates along the z axis and is only permitted to diffract along the x direction, i.e. its intensity $I_2 = I_2(x)$ is assumed to be a function of the x coordinate.

In the following we will essentially retrace the reasoning of [18], but with a somewhat modified model that is closer to the situation of doped photorefractive solids as discussed, e.g.

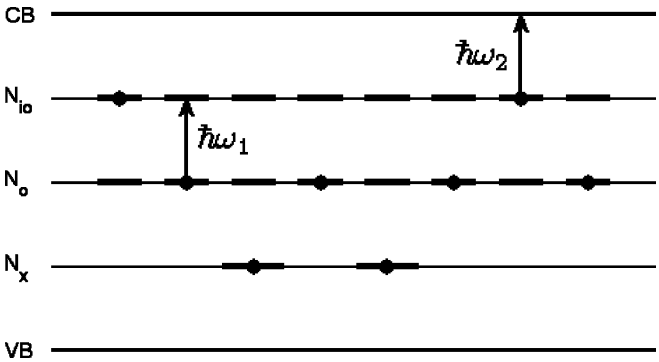

FIGURE 1 Scheme of defect levels and transitions used to model the two-photon photorefractive effect (VB – valence band, N_x – redox levels, CB – conduction band, N_0 – level of electron donating bivalent ions, N_{i0} – intermediate levels)

by Otten et al. [24]. The model assumption is that N_0 bivalent ions have been doped into the crystal and are assumed to be charge compensated. The example we have in mind here, is, e.g. $LiNbO_3$:Fe with the bivalent ions Fe^{2+} and Fe^{3+}. By reduction/oxidation treatments we can preset a specific redox state of the crystal, which is characterized by defect centers, such as oxygen vacancies that act as deep traps. The resulting equilibrium state of the crystal consists in a number of N_x^- electrons per unit volume, permanently captured away from the bivalent ions by these redox centers, in the remaining $N_{\mathrm{D}0} = N_0 - N_x^-$ bivalent ions in the lower valence state (e.g. Fe^{2+}), and in $N_{\mathrm{D}0}^+$ ions in the higher valence state (e.g. Fe^{3+}). In equilibrium, charge conservation implies $N_{\mathrm{D}0}^+ = N_x^-$. Between the ground state of the $N_{\mathrm{D}0}$ ions and the conduction band we place $N_{\mathrm{i}0}$ intermediate levels that can either be realized by excited states of the bivalent ion or other electron accepting states such as color centers, complex oxygen vacancy centers, or centers introduced by double doping with other species of bivalent ions in the oxidized state. The only function relevant in our context is that the $N_{\mathrm{i}0}$ levels (assumed to be charge compensated in equilibrium) can be filled with electrons resulting in N_{i}^- filled intermediate states. The transition scheme of this model is shown in Fig. 1 and is described by the following steady-state rate equations:

$$\gamma_1 N_{\mathrm{i}}^- N_{\mathrm{D}}^+ + \gamma N_{\mathrm{e}} N_{\mathrm{D}}^+ - (s_1 I_1 + \beta_1) N_{\mathrm{D}}\frac{N_{\mathrm{i}}}{N_{\mathrm{i}0}} = 0 \tag{8}$$

$$(s_1 I_1 + \beta_1) N_{\mathrm{D}}\frac{N_{\mathrm{i}}}{N_{\mathrm{i}0}} + \gamma_2 N_{\mathrm{e}} N_{\mathrm{i}} - \gamma_1 N_{\mathrm{i}}^- N_{\mathrm{D}}^+ - (s_2 I_2 + \beta_2) N_{\mathrm{i}}^- = 0\,. \tag{9}$$

Here $\beta_{1,2}$ are the thermal excitation rates, $s_{1,2}$ the cross sections for photoexcitation by photons with energies $\hbar\omega_{1,2}$, and $\gamma_{1,2}$ the relaxation constants between ground state and intermediate level (index 1) and intermediate level and conduction band (index 2), respectively. The relaxation constant between the conduction band and the ground state is denoted by γ, N_{e} is the electron density in the conduction band, N_{D}, N_{D}^+ are the number densities of the bivalent ion that can donate or accept electrons, respectively, N_{i}, N_{i}^- the intermediate levels that are empty or occupied, respectively, and the relationships $N_0 = N_{\mathrm{D}} + N_{\mathrm{D}}^+$ and $N_{\mathrm{i}0} = N_{\mathrm{i}} + N_{\mathrm{i}}^-$ establish their dependence. From (8) and (9) the electron density in the con-

duction band is obtained:

$$N_e = \frac{s_1 I_1 + \beta_1}{[(s_2 I_2 + \beta_2)/N_{i0} + \gamma_1\gamma_2/\gamma]N_i + \gamma_1 N_D^+} \times \frac{(s_2 I_2 + \beta_2) N_D N_i}{\gamma N_D^+ N_{i0}} . \quad (10)$$

In a crystal with sufficiently strong doping we may approximate in first order $N_D \approx N_{D0}$, $N_D^+ \approx N_{D0}^+ = N_x^-$, and $N_i \approx N_{i0}$. In this approximation

$$N_e = N_{e1} \frac{I + b}{I + a + b} , \quad (11)$$

with the dimensionless constants

$$a = \frac{\gamma_1 N_{D0}^+ + \gamma_1\gamma_2 N_{i0}/\gamma}{s_2 I_s} ,$$
$$b = \beta_2/s_2 I_s ,$$

and the photoelectron density

$$N_{e1} = \frac{(s_1 I_1 + \beta_1)}{\gamma} \frac{N_{D0}}{N_{D0}^+}$$

that would have resulted if there were a direct transition into the conduction band. Here we introduced again the dimensionless intensity variable $I(x) = I_2(x)/I_s$ normalized by the supremum $I_s = \sup(I_2(x))$ (i.e. the peak intensity I_s) , so that $0 \le I \le 1$.

In this approximation Poisson's equation is not needed for the description of charge transport. The continuity equation

$$J = e\mu N_e E + eD\frac{\partial N_e}{\partial x} = \text{const.} \quad (12)$$

and Kirchhoff's law

$$\int_{-L/2}^{+L/2} E\,dx + RSJ + V_{ext} = 0 \quad (13)$$

are sufficient. Here e is the elementary charge, μ the mobility, D the electron diffusion coefficient, R and S are resistance and cross section of the external circuit, respectively, and L is the length of the sample in x direction. Since $LiNbO_3$ in principle might exhibit a bulk photovoltaic contribution to the current density, one might wonder why we have omitted such a term in (12). The reason is that the photovoltaic current is connected to electronic transition from suitable centers to the conduction band. But, although we consider photovoltaically active Fe^{2+} donors as an example for our model, note that their transitions transfer electrons to the intermediate level where electrons are localized and thus do not contribute directly to charge transport. On the other hand, the transitions from the intermediate level to the conduction band arise from centers that as a rule are not photovoltaically active.

Usually the experimental situation is such that the external resistance is negligibly small, hence we put $R = 0$. Defining the external field by $E_{ext} = V_{ext}/L$ and the electron density functional $N[I]$ of the intensity by

$$N[I] = \left(\frac{1}{L} \int_{-L/2}^{+L/2} \frac{dx}{N_e(I(x))} \right)^{-1} , \quad (14)$$

the electric field is given by

$$E = -\frac{N[I]}{N_e} E_{ext} - \frac{D}{\mu} \frac{\partial \ln N_e}{\partial x} . \quad (15)$$

In deriving (15) we have assumed that $I(x)$ is a symmetric function of x which is the case for the soliton solutions that we are interested in. Since the diffusion contribution to the electric field is in the order of magnitude of $k_B T/ew$, where $k_B T$ is the thermal energy and w the width of the soliton, it usually can be neglected for solitons at sufficiently strong bias field E_{ext}. The electric field, with this approximation given by:

$$E = -\frac{N[I]}{N_{e1}} \left(1 + \frac{a}{I + b}\right) E_{ext} , \quad (16)$$

induces a perturbation Δn of the refractive index in electro-optic media.

In our case we have $n_0 = n_e$, where n_e is the extraordinary index of refraction,

$$\Delta n = -\frac{n_e^3 r_{33} E}{2} ,$$

and r_{33} is the electro-optic coefficient. This leads to

$$f(I) = \Delta n_0 \frac{N[I]}{N_{e1}} \left(1 + \frac{a}{I + b}\right) . \quad (17)$$

The sign of $\Delta n_0 = 4n_e^2 r_{33} E_{ext}$ depends on the direction of the external field E_{ext} while all other quantities in (17) are positive.

With $F(I) = \Delta n_0 (N[I]/N_{e1})[I + a\ln(I + b)] + gI - \frac{l(l+1)}{I}$ the differential equation for the intensity profile reads as:

$$I' = \pm\sqrt{[F(I) - F(I_\infty)]\, I} . \quad (18)$$

4 Numerical results

From numerical integration one can get solutions that depend on the input parameter $N[I]$. In principle one has then to use (14) to single out the real soliton from these solutions by the requirement of consistency.

However, for grey solitons that have narrow width w compared with the sample dimension L, we may use the approximation $N[I] \approx N_e(I_\infty)$ and hence $N[I]/N_{e1} \approx (I_\infty + b)/(I_\infty + a + b)$ as a first estimate. For $LiNbO_3$ with (see [18, 25]) $n_e = 2.2$, $r_{33} = 3 \times 10^{-11}\,mV^{-1}$, and $E_{ext} = \pm 1.7 \times 10^6\,V\,m^{-1}$ we have $\Delta n_0 = 1 \times 10^{-3}$ for the refractive index change parameter that will be used in the simulations. To estimate the other parameters we use [18, 25]: $\beta_1 = \beta_2 = 1 \times 10^{-20}\,J\,s^{-1}$, $s_1 = s_2 = 1 \times 10^{-6}\,m^2$, $\gamma = \gamma_1 = \gamma_2 = 6 \times 10^{-36}\,J\,m^3 s^{-1}$, $N_{D0} = 1 \times 10^{23}\,m^{-3}$, and $N_{D0}^+ = N_i = 1 \times 10^{22}\,m^{-3}$. This gives $a \approx 10^{-7}\,W\,m^{-2}/I_s$ and $b \approx 10^{-14}$

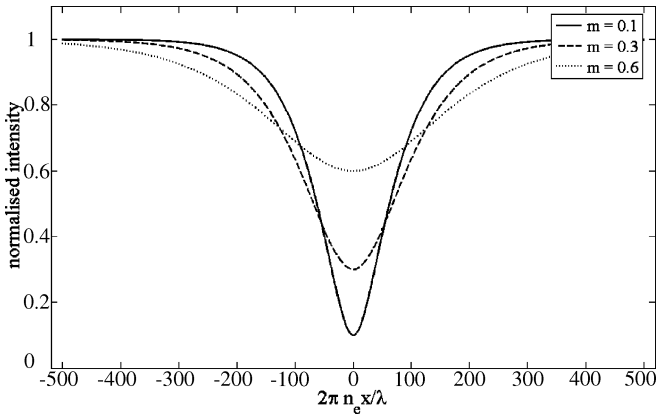

FIGURE 2 Normalized intensity profiles of dark-type grey solitons for $m = 0.1$, 0.3 and 0.6, $\Delta n_0 = 1 \times 10^{-3}$, $a = 100$, $b = 0.01$

$\mathrm{W\,m^{-2}}/I_\mathrm{s}$. Although the parameters of real photorefractive crystals still may deviate by several orders of magnitude from these values, it is plausible that the parameter b will be negligible in most cases. For high power the nonlinearity gets lost since $f(I) \to \Delta n_0 = \text{const.}$ for $a, b \ll 1$, i.e. this is an unfavorable regime for soliton observation. The interesting regime occurs for $a \geq 1$ or $I_\mathrm{s} \leq 10^{-7}\,\mathrm{W\,m^{-2}}$. Intensity profiles for different greyness of dark-type grey solitons parameterized by $m = I_0/I_\infty$ are provided in Fig. 2 for $a = 100$ at $b = 0.01$.

Now we turn to the discussion of incoherently coupled grey solitons in two-photon photorefractive media. For all beams the polarization is assumed to be parallel to the x axis, the propagation direction along the z axis and centered at $x = 0$, and the frequency to be (nearly) the same. The assumption of mutual incoherence of all beams means that the solitons propagate independently but in a refractive index profile created by the total intensity, i.e. the sum of the intensities of all propagating solitons. Hence the amplitude of the ith field fulfills the equation:

$$\left(\frac{1}{2k}\frac{\partial^2}{\partial x^2} + k_0 \Delta n\right)\varphi_i = \Gamma\varphi_i, \quad i = 1, \ldots, N, \tag{19}$$

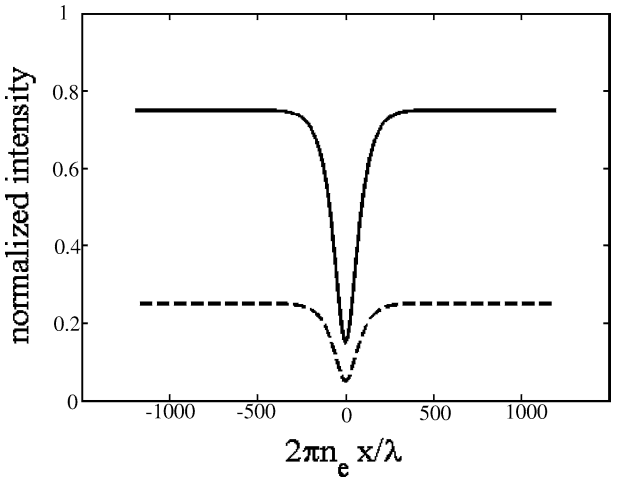

FIGURE 3 Normalized intensity profiles of both components of a grey–grey soliton pair with the parameters $\theta = 30°$, $m = 0.2$, $a = 1.3 \times 10^6$, $b = 0.2$, and $\Delta n_0 = -1.2 \times 10^{-3}$

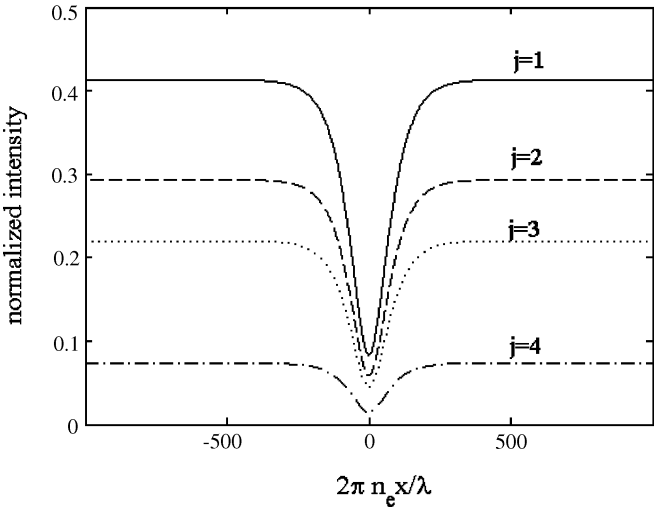

FIGURE 4 Normalized intensity profiles for a soliton consisting of $N = 4$ components with intensities $\alpha_j I_j$, $j = 1, \ldots, 4$ (parameters: $\theta_1 = 40°$, $\theta_2 = 45°$, $\theta_3 = 60°$, $m = 0.2$, $a = 1.3 \times 10^6$, $b = 0.1$, and $\Delta n_0 = -1.2 \times 10^{-3}$)

where the coupling results from dependence of Δn on the total intensity $I_{2,\mathrm{tot}}$, which is the sum of the intensities of all solitons. We describe this total intensity by the supremum I_s and the normalized intensity variable $I = \sum_{j=1}^{N} \alpha_j I_j \leq 1$. Here the individual intensity profiles are given by an intensity variable I_j that is normalized to 1 and the coefficient $\alpha_j = \sin^2\theta_j \prod_{k=0}^{j-1} \cos^2\theta_k$ characterizing the maximum intensity of each of the solitons with $\theta_0 = 0$, appropriately chosen numbers $\theta_1, \ldots, \theta_{N-1}$, and $\theta_N = \pi/2$. For simplicity we choose all I_j to be equal and thus end up with (18) because of the normalization $\sum_{j=1}^{N} \alpha_j = 1$ and hence $I_j = I$. It is obvious that $N = 1$ represents the single soliton case already discussed. We consider therefore now the case $N = 2$, i.e. the case of two overlapping solitons, where $I_1 = I\cos^2\theta$ and $I_2 = I\sin^2\theta$ and θ is an arbitrary projection angle. For a demonstration we have chosen $\theta = 30°$, and $m = 0.2$: Fig. 3 shows a grey–grey pair with the parameters $a = 1.3 \times 10^6$, $b = 0.2$, and $\Delta n_0 = -1.2 \times 10^{-3}$ that correspond to the parameters $\sigma = a/b = 1.3 \times 10^6$, $\varrho = b^{-1} = 5$, and $\beta = (kx_0)^2 \Delta n_0/8 = -178$, respectively, of the paper of Hou et al. [18]. With the same parameters $a = 1.3 \times 10^6$, $b = 0.2$, and $\Delta n_0 = -1.2 \times 10^{-3}$ Fig. 4 depicts the normalized intensity profiles of a multi-component composite grey soliton with $N = 4$ and the parameters $\theta_1 = 40°$, $\theta_2 = 45°$, and $\theta_3 = 60°$, respectively.

5 Conclusion

In conclusion, we have shown that grey solitons, grey–grey soliton pairs, and multi-component grey solitons can be realized in two-photon photorefractive media under steady-state conditions. In the derivation we have presupposed that the carrier beams share the same polarization and wavelength, and are mutually incoherent.

ACKNOWLEDGEMENTS This work was supported by the National Natural Science Foundation of China (No. 10474136), by the

Austria/China Mobility Program (project VII. B.7), and by the FWF project P-18988.

REFERENCES

1 M. Segev, B. Crosignani, A. Yariv, B. Fischer, Phys. Rev. Lett. **68**, 923 (1992)
2 D.N. Christodoulides, M.I. Carvalho, Opt. Lett. **19**, 1714 (1994)
3 M. Segev, G.C. Valley, B. Crosignani, P. Diporto, A. Yariv, Phys. Rev. Lett. **73**, 3211 (1994)
4 D.N. Christodoulides, M.I. Carvalho, J. Opt. Soc. Am. B **12**, 1628 (1995)
5 M. Segev, M. Shih, G.C. Valley, J. Opt. Soc. Am. B **13**, 706 (1996)
6 M.D. Iturbe-Castillo, P.A. Marquez-Aguilar, J.J. Sanchez-Mondragon, S. Stepanov, V. Vysloukh, Appl. Phys. Lett. **64**, 408 (1994)
7 G.C. Valley, M. Segev, B. Crosignani, A. Yariv, M.M. Fejer, M.C. Bashaw, Phys. Rev. A **50**, R4457 (1994)
8 M. Segev, G.C. Valley, M.C. Bashaw, M. Taya, M.M. Fejer, J. Opt. Soc. Am. B **14**, 1772 (1997)
9 S. Bian, J. Frejlich, K.H. Ringhofer, Phys. Rev. Lett. **78**, 4035 (1997)
10 Z. Chen, M. Segev, D.W. Wilson, R.E. Muller, P.D. Maker, Phys. Rev. Lett. **78**, 2948 (1997)
11 L. Keqing, T. Tiantong, Z. Yanpeng, Phys. Rev. A **61**, 053 822 (2000)
12 L. Keqing, Z. Yanpeng, T. Tiantong, J. Opt. A Pure Appl. Opt. **3**, 262 (2001)
13 E. Fazio, F. Renzi, R. Rinaldi, M. Bertolotti, M. Chauvet, W. Ramadan, A. Petris, V.I. Vlad, Appl. Phys. Lett. **85**, 2193 (2004)
14 M. Segev, A.J. Agranat, Opt. Lett. **22**, 1299 (1997)
15 E. DelRe, M. Tamburrini, M. Segev, E. Refaeli, A.J. Agranat, Appl. Phys. Lett. **73**, 16 (1998)
16 A. Stepken, E. Kaiser, M.R. Belić, J. Opt. Soc. Am. B **17**, 68 (2000)
17 A.V. Mamaev, M. Saffman, D.Z. Anderson, A.A. Zozulya, Phys. Rev. A **54**, 870 (1996)
18 C. Hou, Y. Pei, Z. Zhou, X. Sun, Phys. Rev. A **71**, 053 817 (2005)
19 A.G. Grandpierre, D.N. Christodoulides, T.H. Coskun, M. Segev, Y.S. Kivshar, J. Opt. Soc. Am. B **18**, 55 (2001)
20 D.N. Christodoulides, S.R. Singh, M.I. Carvalho, M. Segev, Appl. Phys. Lett. **68**, 1763 (1996)
21 Z. Chen, M. Segev, T.H. Coskun, D.N. Christodoulides, Y.S. Kivshar, J. Opt. Soc. Am. B **14**, 3066 (1997)
22 L. Keqing, Z. Yanpeng, T. Tiantong, L. Bo, Phys. Rev. E **64**, 056 603 (2001)
23 S. Bugaychuk, L. Kovacs, G. Mandula, K. Polgar, R.A. Rupp, Phys. Rev. E **67**, 046 603 (2003)
24 J. Otten, A. Bledowski, K.H. Ringhofer, R.A. Rupp, Comput. Phys. Commun. **69**, 187 (1992)
25 E. Castro-Camus, L.F. Magaña, Opt. Lett. **21**, 1129 (2003)